Slow-light dispersion by transparent waveguide plasmon polaritons

Atsushi Ishikawa,[1,2] Rupert F. Oulton,[1,3] Thomas Zentgraf,[1,4] and Xiang Zhang[1,5]

[1]*NSF Nanoscale Science and Engineering Center, University of California, 3112 Etcheverry Hall, Berkeley, California 94720, USA*

[2]*Metamaterials Laboratory, RIKEN, 2-1 Hirosawa, Wako, Saitama 351-0198, Japan*

[3]*Experimental Solid State Physics, The Blackett Laboratory, Imperial College London, London SW7 2BZ, United Kingdom*

[4]*Department of Physics, University of Paderborn, Warburger Straße 100, D-33098 Paderborn, Germany*

[5]*Materials Sciences Division, Lawrence Berkeley National Laboratory, Berkeley, California 94720, USA*

(Received 31 May 2011; revised manuscript received 30 January 2012; published 5 April 2012)

We propose a classical analogue of electromagnetically induced transparency for a two-level ensemble interacting with two orthogonal optical modes. We show that a single localized plasmon resonance of a metal nanoparticle ensemble coupled to counter-propagating modes of a dielectric waveguide generates a slow transparent waveguide-plasmon polariton. Dispersion is controllable by tuning the coupling strengths of localized plasmon and waveguide modes, while maintaining extremely low loss at the system's transparency. Strong coupling in such plasmonic hybrid systems leads to large group index-bandwidth products.

DOI: 10.1103/PhysRevB.85.155108 PACS number(s): 73.20.Mf, 78.20.Ci, 42.70.Qs, 42.50.Gy

I. INTRODUCTION

Electromagnetically induced transparency (EIT) is an important phenomenon in quantum optics for its capability to slow down and even stop light[1] with potential applications in all-optical memories,[2] and enhanced optical nonlinearity.[3] Quantum interference of electronic levels in an atomic ensemble, addressed by optical pump and probe fields, creates a highly dispersive response leading to a large group index of the probe field.[4] Recently, a number of reports have discussed classical analogues of EIT arising from the selective coupling of multiple photonic elements with an optical field.[5–12] Although this is a static phenomenon due to wave interference, such systems exhibit the same highly dispersive responses as in atomic ensembles.

In this letter, we propose a physical mechanism for achieving a classical EIT effect for a two-level ensemble interacting with two orthogonal optical modes. We show that a simple periodic ensemble of resonant metal nanoparticles within a dielectric waveguide supports a transparent waveguide-plasmon polariton (WPP) mode for guided slow-light propagation. Such systems inherit the strongly dispersive properties of the nanoparticles embedded in the waveguide, but do not succumb to the associated absorptive losses by utilizing the system's transparency.

A schematic of atomic EIT is shown in Fig. 1(a), where a probe field, $|1\rangle$, addresses a three-level atom in a Λ configuration and drives the atomic transition $\omega_{e_1 g}$ between the ground $|g\rangle$ and excited states $|e_1\rangle$. Coupling to a second atomic transition $\omega_{e_1 e_2}$ requires a different frequency pump field $|2\rangle$. Coupling between the ground and lower excited states is not allowed. Atomic EIT occurs for a nonzero pump field allowing mutual coupling of all states and inducing destructive quantum interference of the probe field's absorption via the $\omega_{e_1 g}$ transition.

The classical analogue of EIT, on the other hand, can be understood as a frequency-degenerate version of atomic EIT where the effect is always "on," i.e., $\omega = \omega_{e_1 g} = \omega_{e_1 e_2}$. The effect is common to linear systems where the interaction of two orthogonal modes is mediated by a third. When all underlying modes are degenerate, the zero frequency splitting normal mode is a linear combination of just the two orthogonal underlying modes; the third mode is not excited and is essentially "transparent" within the coupled system.[13] Recently, classical analogues of EIT have been demonstrated in coupled plasmonic or photonic resonators.[6,14,15] However, these approaches exploit just one of two possible configurations [see Fig. 1(b) left] where the two resonator ground states are orthogonal $\langle g|e_2\rangle = 0$, and the external optical field couples predominantly to just one of the resonators. In this letter, we propose a different approach [see Fig. 1(b) right], where the two ground states are one and the same, $|g\rangle = |e_2\rangle$ (i.e., a two-level system), but the pump and probe beams are now orthogonal $\langle 1|2\rangle = 0$. This is so appealing because it only requires a single two-level optical resonance, which greatly simplifies the complexity of conventional classical EIT approaches and allows for wide tunability. Note that we still interpret this as a three-level classical analogue of EIT, only with mode selectivity working in addition to the resonator to define the three levels.

II. THEORETICAL DESCRIPTION

Here, we demonstrate this approach for a multi-mode silicon waveguide coupled to a plasmonic resonator array, shown in Fig. 1(c). Each nanoparticle exhibits a localized plasmon (LP) resonance near the telecom frequency with dipole orientation along the z axis. The nanoparticles' extinction spectrum and $|E|^2$ distribution near resonance ω_{lp} are shown in Fig. 1(d). The calculations are performed using the finite-element-method (FEM) with $n_{\mathrm{si}} = 3.53$, $n_{\mathrm{sio2}} = 1.45$, and the empirical value for n_{Ag}.[16] An incident fundamental transverse magnetic mode (TM_0) is resonantly scattered by the LP mode and couples to either backward travelling TM_0 or TM_1 modes, depending on the resonator period Λ. A WPP occurs when all three modes (LP and two waveguide modes) are degenerate at the points (i) or (ii) in Fig. 1(e).

The coupling of LP-TM_m-TM_n modes near a degeneracy point is described by a matrix equation based on the effective

Hamiltonian:[17]

$$\left[\begin{pmatrix} \omega_0 - v_{gn}\Delta k & 0 & C_n \\ 0 & \omega_0 + v_{gm}\Delta k & C_m \\ C_n & C_m & \omega_0 + \delta + i\gamma \end{pmatrix} - \Omega\right]\begin{pmatrix} \psi_n \\ \psi_m \\ \psi_{lp} \end{pmatrix} = 0, \tag{1}$$

where ω_0 is the frequency at the point (i) or (ii), the two modal propagation constants are related to the resonator period by $\beta_m(\omega_0) = 2\pi/\Lambda - \beta_n(\omega_0) = k_{z0}$, $\Delta k = k_z - k_{z0}$. $v_{gi} = c/n_{gi}$ ($i = m$ or n) are the "local" group velocities of the waveguide modes that approximate a linear mode dispersion near ω_0 and k_{z0}, C_i are mode coupling strengths to the LP mode, $\delta = \omega_{lp} - \omega_0$ is the detuning of LP mode, and $[m, n]$ takes [1, 0] or [0, 0] for the point (i) or (ii), respectively. The solution of Eq. (1) at k_{z0} gives three eigenfrequencies: $\Omega_0 = \omega_0$ and $\Omega_\pm = \omega_0 + (\delta + i\gamma)/2 \pm \sqrt{(\delta + i\gamma)^2/4 + C_m^2 + C_n^2}$. The eigenvector of the transparency mode, $\psi_0 = (C_m - C_n\, 0)(C_m^2 + C_n^2)^{-1/2}$, is a superposition of waveguide modes only, i.e., the plasmonic resonance is cancelled out. The other two modes define the upper and lower edges of the coupling induced band gap of the system. Transparent WPPs arise from the system's periodicity and are independent of the nanoparticles' resonant properties since the WPP's eigenfrequency is independent of their detuning δ. Only the relative coupling strengths and the group velocities control the peak WPP group velocity at k_{z0},

$$v_g(\omega_0) = \frac{\partial\Omega_0(k_{z0})}{\partial k_z} = \frac{v_{gm}C_n^2 - v_{gn}C_m^2}{C_m^2 + C_n^2}. \tag{2}$$

The system's insensitivity to the resonators' detuning means it should be robust against variations in the resonator size and would be sensitive only to variations in periodicity, making the observation of transparent WPPs practically possible.

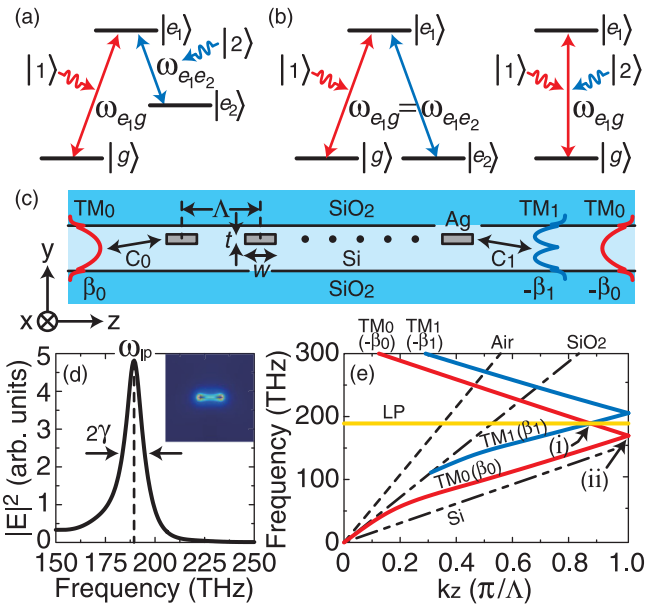

FIG. 1. (Color online) Schematics of (a) atomic EIT and (b) classical analogues. (c) Plasmonic resonator ($w/t = 50/5$ nm) array embedded in a silicone waveguide with the core thickness of 600 nm. (d) $|E|^2$ spectral response of probe placed 5 nm from the resonator's end facet and $|E|^2$ distribution of LP mode at resonance, $\omega_{lp}/2\pi =$ 189 THz. (e) Numerically calculated dispersion relations of TM_0 and TM_1 bare modes for $\Lambda = 275$ nm. Coupled LP-TM_0-TM_1 modes occur at the degeneracy point (i). When Λ is set at 240 nm, coupled LP-TM_0-TM_0 modes occur at the point (ii).

III. RESULTS AND DISCUSSION

Figure 2(a) shows dispersion relations for coupled LP-TM_0-TM_1 modes based on Eq. (1) with various coupling strengths, while Fig. 2(b) shows the central WPP's retrieved group index. Figures 2(c) and 2(d) show the same information for the LP-TM_0-TM_0 case with different detunings. To simplify the problem, initially we have assumed $\gamma = 0$, $n_{g0} = 3.8$, $n_{g1} = 4.5$, $\beta_0 = 3.33\omega_0/c$, and $\beta_1 = 2.47\omega_0/c$ at $\omega_0/2\pi =$ 189 THz for solving Eq. (1). For the coupling of different mode orders, the slow-light condition is attained by tuning the coupling strengths, as shown in Figs. 2(a) and 2(b). The highest possible group index, as per Eq. (2), requires different coupling strengths to compensate for the difference in the mode group velocities, such that $C_m/C_n = \sqrt{v_{gm}/v_{gn}}$.

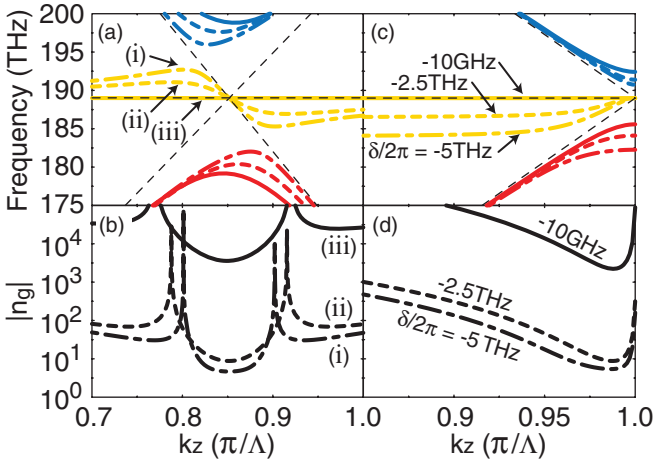

FIG. 2. (Color online) (a) Dispersion relations of coupled LP-TM_0-TM_1 modes based on Eq. (1), and (b) central WPP's retrieved group index. (c) and (d) are the same for the LP-TM_0-TM_0 case with different detunings. In (a) and (b), δ and $\gamma = 0$ for all and the coupling strengths are (i) $\hbar[C_0, C_1] = [10, 30]$ meV, (ii) $\hbar[C_0, C_1] =$ [20,30] meV, and (iii) $\hbar[C_0, C_1] = [30, 27.6]$ meV. In (c) and (d), $\hbar C_0 = 10$ meV and $\gamma = 0$ for all.

This is achievable by adjusting the resonator position in the waveguide core along the y-axis using the different field distributions of TM_0 and TM_1 modes, as shown in Fig. 1(c). The condition is implicit for coupling between the same mode orders with a vanishing WPP group velocity $v_g(\omega_0) \to 0$.

The group velocity for a WPP remains slow within a bandwidth $\Delta\omega = \Omega_0 - \omega_0$ with a group index, $n_g(\omega) = \Re[c/v_g(\omega)]$, given by

$$n_g(\omega) \approx \frac{c[v_g(\omega_0) + \kappa\Delta k\delta]}{[v_g(\omega_0) + \kappa\Delta k\delta]^2 + \kappa^2\Delta k^2\gamma^2}, \tag{3}$$

where $\kappa \approx 2v_{gm}v_{gn}/(C_m^2 + C_n^2)$. For coupled LP-$TM_0$-$TM_1$ modes, WPP dispersion is approximately linear near k_{z0}, where $\Delta\omega = v_g(\omega_0)\Delta k$. Here, the group index peaks at ω_0 and has a full width half maximum bandwidth of $v_g(\omega_0)/\kappa\sqrt{\delta^2 + \gamma^2}$. Enhancement of the group index is achieved through the quadratic dependence on the coupling strength and by minimizing both the resonator losses and detuning.

For coupled LP-TM_0-TM_0 modes, the peak group index is asymptotic near ω_0 with a quadratic dispersion near the band edge. In the case of plasmonic resonators, one would expect $\gamma \gg \delta$, thus $n_g(\omega) \approx n_{g0}C_0/2\sqrt{\Delta\omega\gamma}$. Here, quadratic dispersion renders a linear dependence between group index and coupling strength, so narrow bandwidths will accompany high group indexes. In this example, group indexes in excess of 100 are achievable at a frequency of 200 THz with bandwidths < 10 GHz. However, for atomic systems where $\gamma \ll \delta$, the group index, $n_g(\omega) \approx n_{g0}C_0/\sqrt{2\Delta\omega\delta}$, is limited by the resonators' detuning and larger slow-light bandwidths are achievable, as indicated in Fig. 2(d).

Figure 3(a) shows numerically calculated dispersion relations for coupled LP-TM_0-TM_1 modes with resonators positioned 123 nm above the waveguide core's center. The three hybridized normal modes [red $\Re(\Omega_-)$, yellow $\Re(\Omega_0)$, and blue $\Re(\Omega_+)$ curves] closely follow the analytical results (dashed curves) based on Eq. (1). The lowest and highest modes (orange and green curves) originate from the lower TM_0 and upper TM_1 modes, respectively. Figure 3(b) shows the damping frequencies (loss per unit time) of the middle three modes and the retrieved group index of the central mode (black curve). At $k_z\Lambda/\pi = 0.86$, the loss of the WPP drops drastically by $\sim$4 orders of magnitude, corresponding to $2k_{Im} = 2n_g\omega_{Im}/c \approx 0.9$ dB/cm, whereas the other normal modes become extremely lossy as they hybridize with the LP mode. Since $C_0 > C_1$, the WPP character is more TM_0 like, propagating slowly ($n_g = 13.6$) toward the positive z direction. Moving the resonators to 130 nm above the core's center, we approach $C_1/C_0 = \sqrt{v_{g1}/v_{g0}}$ where the group index increases to 98.3 (dashed curve), without increasing mode loss.

Figure 3(c) shows $|E|^2$ distributions of the middle three modes (ψ_-, ψ_0, and ψ_+) at $k_z\Lambda/\pi = 0.86$, labeled as (i), (ii), and (iii) in Fig. 3(a). For ψ_0 [(ii) of Fig. 3(c)], the interference between counter-propagating TM_0 and TM_1 modes forms a standing wave, cancelling out the electric field at the resonator. As a result, the WPP exhibits both slow-light and low-loss properties simultaneously. Conversely, the resonators light up

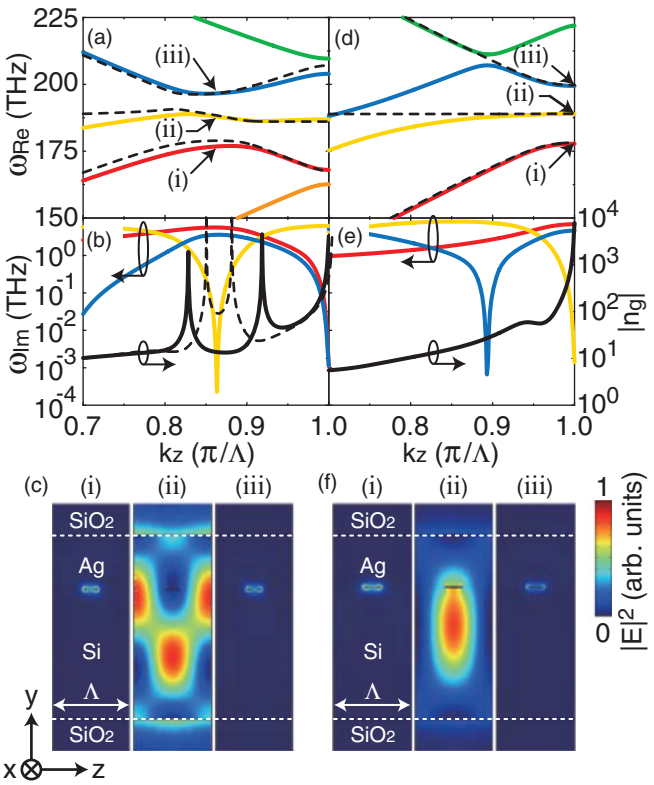

FIG. 3. (Color online) (a) Numerically calculated dispersion relations for coupled LP-TM_0-TM_1 modes with resonators located 123 nm above the waveguide core's center. Numerical dispersion agrees with analytical one from Eq. (1) (dashed curves) using $\hbar[C_0, C_1] = [28, 37]$ meV, $\delta/2\pi = -100$ GHz, and $2\gamma/2\pi = 10.5$ THz. (b) Damping rates of the middle three modes (red, yellow and blue curves) and the retrieved group index of the central mode (black curve). Dashed curve is the group index when Eq. (2) is satisfied (resonator position at 130 nm above the core's center). (c) $|E|^2$ distributions of the middle three modes at $k_z\Lambda/\pi = 0.86$, labeled as (i), (ii), and (iii) in (a). (d), (e), and (f) show the LP-TM_0-TM_0 case with resonators located 130 nm above the core's center. The analytical dispersion (dashed curves) uses $\hbar C_0 = 35$ meV, $\delta/2\pi = -100$ GHz, and $2\gamma/2\pi = 10.5$ THz. (f) $|E|^2$ distributions of the lower three modes at $k_z\Lambda/\pi = 1.0$, labeled as (i), (ii), and (iii) in (d). Note that $|E|^2$ distributions of mode (ii) in (c) and (f) have been multiplied by 100 and 25, respectively, for clarity.

for ψ_- and ψ_+ since they hybridize the LP mode [(i) and (iii) of Fig. 3(c)].

Figures 3(d) and 3(e) show similar calculations for coupled LP-TM_0-TM_0 modes. Here, the mode coupling symmetry leads to slow-light behavior at the band edge with quadratic dispersion even when $\delta \neq 0$. As a result, the WPP exhibits an asymptotically large group index with very low mode loss. Note the second transparent WPP (blue curve) for the detuned coupled LP-TM_0-TM_1 modes. Figure 3(f) shows $|E|^2$ distributions of the lower three modes at the band edge, labeled as (i), (ii), and (iii) in Fig. 3(d). The WPP is a standing wave of interfering counter-propagating TM_0 modes. The E_z field, which excites the LP mode, is totally cancelled at the resonator, while the finite E_y field leads to modest absorption loss.

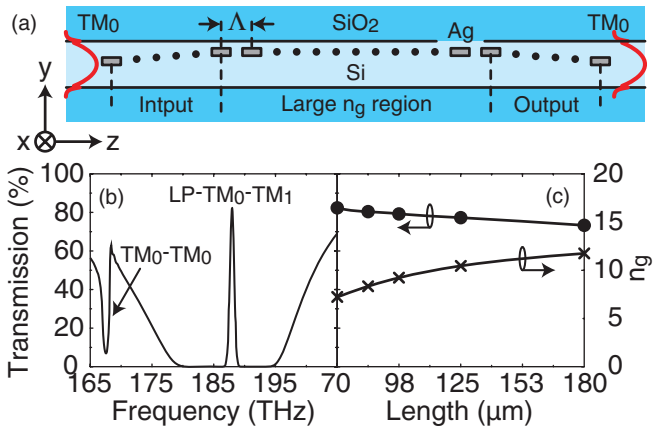

FIG. 4. (Color online) (a) A slow-light waveguide made of a large group-index region sandwiched between coupling regions. The large group-index region has 0–400 resonators located 123 nm above the core's center, while the coupling regions have 125 resonators each with the y position gradually changed from 70 to 123 nm for adiabatic coupling. (b) Transmission spectra through the waveguide with a length of 70.75 μm. (c) Waveguide length dependence of transmission and averaged group index of the system.

IV. APPLICATION TO SLOW-LIGHT WAVEGUIDES

Naturally, the LP-TM_0-TM_0 system is preferable for maximally slowing down light. Efficient coupling to this band-edge WPP from the outside may be achieved using slow-wave injectors,[18] but the slow-light bandwidth is impractically narrow. Alternatively, the semiconductor platform is ideal for exploiting nonlinearities toward achieving a dynamic system response; e.g., mode group velocities and their coupling to the plasmonic resonators could be controlled through electro-optic modulation.[19] Furthermore, such a system could be electrically addressed through the metal nanoparticle array. Here, we explore the asymmetric LP-TM_0-TM_1 WPP with adiabatic couplers for a large group index-bandwidth product (GBP). Figure 4(a) is a slow-light waveguide where a large group-index region is sandwiched between adiabatic input and output regions. The change in resonator position tunes the relative coupling strengths of the TM_0 and TM_1 modes to the LP mode effectively impedance matching the light as it is slowed down.[20–22]

Figure 4(b) shows transmission spectra through the waveguide with just the coupling regions of length 70.75 μm (total 250 resonators). The transparent WPP is clearly visible in the band gap of coupled LP-TM_0-TM_1 modes. Figure 4(c) shows the waveguide length dependence of transmission and averaged group index of the system. As the length increases, the transmission decreases very slowly due to millimeter range mode propagation, while the group index increases to 11.8 at 180 μm, approaching the theoretical value of 13.6 in Fig. 3(b). Higher group indexes are achievable by adjusting the coupling strengths, as suggested in Fig. 3(b).

Finally, let us discuss the advantages of the proposed system in terms of their GBP,[23] expressed as

$$n_g \frac{\Delta\omega}{\omega_0} = \frac{n_{gm} C_n^2}{\omega_0^2} \left(\frac{C_m^2}{C_n^2} - \frac{v_{gm}}{v_{gn}} \right) \frac{Q}{\sqrt{\delta^2/\gamma^2 + 1}}, \qquad (4)$$

where $Q = \omega_{lp}/2\gamma$ is the resonators quality factor. For the system shown in Fig. 4(a), the GBP is 0.098 ($\Delta\omega/2\pi$ = 1.57 THz), which is in good agreement with the predicted value of 0.094 based on Eq. (4) with the fitting constants in Fig. 3(a). This is sufficient to store 11 sub-ps pulses in a distance of 180 μm and comparable to that of photonic crystal systems.[24] Interestingly, the GBP varies quadratically with the coupling strengths but only linearly with the quality factor. While any type of photonic resonators may achieve a similar effect, plasmonic ones are appealing due to much stronger light-resonator coupling despite relatively low quality factors, leading to superior GBPs for compact slow-light devices.

V. CONCLUSION

We have presented a physical mechanism of classical EIT arising from the interaction of plasmonic resonators with two counter-propagating modes in a dielectric waveguide. In this scheme, there is no need to combine multiple optical resonators to create the effect, simplifying the practical implementation of the classical EIT effect. Furthermore, light propagation through the system provides extremely strong dispersion from the resonators but suffers very low propagation loss by exploiting the system's transparency. Hence this approach may open up new avenues for achieving highly dispersive low-loss propagation in nanoplasmonic structures.

ACKNOWLEDGMENTS

This work is financially supported by the National Science Foundation Nano-scale Science and Engineering Center (NSF-NSEC) for Scalable and Integrated NAnoManufacturing (SINAM) (Grant No. CMMI-0751621). A.I. is supported by the RIKEN Special Postdoctoral Researcher Program. R.F.O. is supported by an EPSRC Fellowship (EP/I004343/1) and Marie Curie IRG (PIRG08-GA-2010-277080).

[1] S. E. Harris, Phys. Today **50**, 36 (1997).
[2] D. F. Phillips, A. Fleischhauer, A. Mair, R. L. Walsworth, and M. D. Lukin, Phys. Rev. Lett. **86**, 783 (2001).
[3] S. E. Harris, J. E. Field, and A. Imamoglu, Phys. Rev. Lett. **64**, 1107 (1990).
[4] K. J. Boller, A. Imamoglu, and S. E. Harris, Phys. Rev. Lett. **66**, 2593 (1991).
[5] D. D. Smith, H. Chang, K. A. Fuller, A. T. Rosenberger, and R. W. Boyd, Phys. Rev. A **69**, 063804 (2004).
[6] S. Zhang, D. A. Genov, Y. Wang, M. Liu, and X. Zhang, Phys. Rev. Lett. **101**, 047401 (2008).
[7] H.-C. Liu and A. Yariv, Opt. Express **17**, 11710 (2009).
[8] T. Zentgraf, S. Zhang, R. F. Oulton, and X. Zhang, Phys. Rev. B **80**, 195415 (2009).

[9]N. Papasimakis, V. A. Fedotov, N. I. Zheludev, and S. L. Prosvirnin, Phys. Rev. Lett. **101**, 253903 (2008).
[10]P. Tassin, L. Zhang, T. Koschny, E. N. Economou, and C. M. Soukoulis, Phys. Rev. Lett. **102**, 053901 (2009).
[11]N. Liu, L. Langguth, T. Weiss, J. Kästel, M. Fleischhauer, T. Pfau, and H. Giessen, Nat. Mater. **8**, 758 (2009).
[12]R. D. Kekatpure, E. S. Barnard, W. Cai, and M. L. Brongersma, Phys. Rev. Lett. **104**, 243902 (2010).
[13]B. Luk'yanchuk, N. I. Zheludev, S. A. Maier, N. J. Halas, P. Nordlander, H. Giessen, and C. T. Chong, Nat. Mater. **9**, 707 (2010).
[14]Q. Xu, S. Sandhu, M. L. Povinelli, J. Shakya, S. Fan, and M. Lipson, Phys. Rev. Lett. **96**, 123901 (2006).
[15]K. Totsuka, N. Kobayashi, and M. Tomita, Phys. Rev. Lett. **98**, 213904 (2007).
[16]P. B. Johnson and R. W. Christy, Phys. Rev. B **6**, 4370 (1972).
[17]A. Christ, S. G. Tikhodeev, N. A. Gippius, J. Kuhl, and H. Giessen, Phys. Rev. Lett. **91**, 183901 (2003).
[18]P. Velha, J. P. Hugonin, and P. Lalanne, Opt. Express **15**, 6102 (2007).
[19]A. Liu, R. Jones, L. Liao, D. Samara-Rubio, D. Rubin, O. Cohen, R. Nicolaescu, and M. Paniccia, Nature (London) **427**, 615 (2004).
[20]T. Baba, D. Mori, K. Inoshita, and Y. Kuroki, IEEE J. Sel. Top. Quantum Electron. **10**, 484 (2004).
[21]D. Mori and T. Baba, Appl. Phys. Lett. **85**, 1101 (2004).
[22]Y. A. Vlasov and S. J. McNab, Opt. Lett. **31**, 50 (2006).
[23]T. Baba, Nat. Photonics **2**, 465 (2008).
[24]J. Li, T. P. White, L. O'Faolain, A. Gomez-Iglesias, and T. F. Krauss, Opt. Express **16**, 6227 (2008).